Tensile Properties of Polypropylene Composites Reinforced with Alumina Nanoparticles and Short Carbon Fibers

*João Lucas A.N.G. Ferreira[a]** [ID], *Marisa Cristina G. Rocha[a]* [ID]

[a]Universidade do Estado do Rio de Janeiro (UERJ), Instituto Politécnico (IPRJ), Nova Friburgo, RJ, Brasil.

The good properties and high productivity obtained through injection molding have enabled the use of composites reinforced with short carbon fibers for the production of automobile components. Their low strength and stiffness, however, have limited the use of these materials in some applications. The incorporation of inorganic nanoparticles such as alumina (Al_2O_3) is a proposed solution to this problem. There is evidence that nanoparticles promote better interfacial interaction between the polymer and short carbon fibers, improving the mechanical performance of composites. The aim of this work was to develop polypropylene (PP) composites reinforced with alumina nanoparticles and short carbon fibers for the automotive industry. The composites were processed in a twin-screw extruder. The response surface methodology was used to define the content of nanoparticles in the composites and to evaluate the effect of the incorporation of the alumina and polypropylene-grafted maleic anhydride (PP-g-MA) on the properties obtained. The hybrid composite that showed the best tensile properties was used as a matrix for reinforcement with different levels of short carbon fiber. The tensile properties were determined by the standard techniques. The results showed that the materials obtained can be used in applications that require low density along with high productivity, rigidity and resistance.

Keywords: *Polypropylene, Hybrid composites, Short carbon fibers, Alumina.*

1. Introduction

Composites are materials that have two or more chemically different constituents and that on the macroscopic scale have a well-defined interface. In general, these materials have better properties than their constituent elements[1,2]. The properties of these materials are a function of the properties of the constituent phases, their relative concentrations and the shape, size, distribution and orientation of the particles in the dispersed phase[1,2].

Nowadays, there is increasing use of polymeric thermoplastic composites in the automotive industry, since they make cars lighter and promote greater fuel/energy efficiency[3]. The cost and strength of these materials depend on the manufacturing process. Despite their high mechanical performance, continuous fibers cannot be processed through injection molding, which makes the mass production of these composites difficult[3]. As a result, there is a growing tendency to use short fibers as reinforcing elements in thermoplastic matrices, due to the high productivity obtained through the injection molding process and the recyclability. However, these materials have low stiffness and strength compared to thermosetting polymer matrix composites, even when high strength fibers such as carbon fibers are used. The strength of these materials is a function of the fiber length and content, as well as the interfacial shear strength, which is very low between polypropylene and carbon fibers[3].

The addition of nanoparticles to composites filled with fiber-reinforced thermoplastic matrices is an interesting alternative to obtain superior properties without changing the processing conditions, as long as there is a good distribution and dispersion of the nanoparticles among the fibers. In addition to improving the properties of the matrix, nanoparticles also affect the interfacial adhesion between the filler and matrix. There are reports in the literature indicating that the incorporation of nanofillers improves some properties of short fiber reinforced thermoplastic composites[3-8].

Arao et al.[3] reported that hybrid polypropylene (PP) composites consisting of polypropylene grafted with maleic anhydride (PP-g-MA), different types of nanofillers (alumina, silica, carbon nanotubes (CNT)) and short carbon fibers (SCF) have better mechanical properties than PP/SCF composites. Fiber pullout tests and observation of the fracture surface of the hybrid composites indicated that the nanoparticles increased the interfacial shear strength (IFFS) between PP and carbon fibers, which is extremely low, improving the mechanical performance of the materials obtained.

Junaedi et al.[6] demonstrated that the incorporation of graphite-nanoplatelets (GNP) increased the interfacial strength between short carbon fibers and the polypropylene matrix. The 85/10/5 PP/SCF/GNP composite showed Young`s modulus and ultimate tensile strength (UTS) approximately 27% and 20% higher than those presented by the PP/10 SCF composites.

Some published papers also shown that the use of low levels of compatibilizers, such as PP-g-MA, can improve the interfacial adhesion between the polymer and the fibers[3,4]. Good wettability of the fibers is essential to avoid gaps between the fibers and the solidified matrix, improving the interfacial

*e-mail: joaolucasgalvao@gmail.com

adhesion and promoting better mechanical behavior of the composites[9]. In the absence of compatibilizers, there is low wettability of carbon fibers by the PP matrix[10]. In general, since the compatibilizer generally has low molecular weight, the wettability of the matrix increases with rising compatibilizer content[9]. Furthermore, the carbon fibers are oxidized, in addition to other surface treatments, in order to promote the chemical bonding between the maleic anhydride groups and the surface of the fibers, which contains some functional groups, such as hydroxyl groups[11,12].

The incorporation of alumina nanoparticles in thermoplastic matrices is a strategy used to improve their properties[3,4].

The response surface methodology (RSM) is an efficient means of determining the optimal formulation of a specific mixture. The measured response depends only on the relative proportions of the components in the mixture[13-16]. The objective of this work was to use the RSM methodology to develop hybrid polypropylene composites reinforced with alumina nanoparticles and short carbon fibers.

2. Materials and Methods

2.1. Materials

Braskem SA furnished the polypropylene (PP, H503), with melt flow index (MFI) = 3.5 g/10 min – ASTM D1238[17].

Chemtura Industria Quimica do Brasil supplied the polypropylene grafted with maleic anhydride (PP-g-MA, Polybond 3200), with MFI = 115 g/10 min – ASTM D 1238[17], at 190 °C.

Sigma-Aldrich supplied the calcined alumina (Al_2O_3) on nanometer scale (13 nm).

Parabor kindly donated short carbon fibers from Toho Tenax America, under the trade name Tenax®-A/J HT C804, with an average length of 6 mm, diameter (D) of 7 μm and specific mass of 1.8 g /cm³.

BASF supplied the antioxidant Irganox® 1010 FF.

Ciba Especialidades Químicas Ltda supplied Atmer SA 1753 calcium stearate, the compound used as a lubricant in the processing of materials in a single-screw extruder.

2.2. Methods

2.2.1. Experimental design of mixtures

The response surface methodology consists of fitting a polynomial mathematical model to a response surface that is obtained according to a specific experimental design (design of experiment – DOE), known as a statistical mixture design. The content of each component of the mixture can vary between zero and one, and the sum of all components is equal to one. The experimental region of a mixture composed of three components is a triangle defined by the coordinates (0, 0, 1), (0, 1, 0) and (1, 0, 0). The vertices of the triangle correspond to each of the three constituents of the mixture; the sides of the triangle correspond to binary mixtures; and the points located inside the triangle represent the ternary mixtures[13-16].

In this work, the Minitab 19 software was used for the experimental design of the mixtures. This software was also used to describe the tensile mechanical behavior of

the samples. Polypropylene, alumina and PP-g-MA were represented by input variables designated as PP, Al_2O_3 and PP-g-MA, respectively.

The content of compatibilizer and alumina nanoparticles initially adopted was 4%, based on published studies[3,18]. However, preliminary results obtained using the response surface methodology showed that better tensile properties of the composites could be obtained using a wider range of concentration of these constituents. Therefore, the components of the mixture were submitted to the following restrictions: $0.88 \leq PP \leq 1.0$, $0 \leq Al_2O_3 \leq 0.06$ and $0 \leq PP\text{-}g\text{-}MA \leq 0.06$. Figure 1 shows the project's region of interest. The circles represent nine PP/PP-g-MA/Al_2O_3 mixtures, which must be prepared to generate an adequate response surface using an n-degree polynomial equation. Table 1 shows the composition of the materials under study defined by the Minitab software.
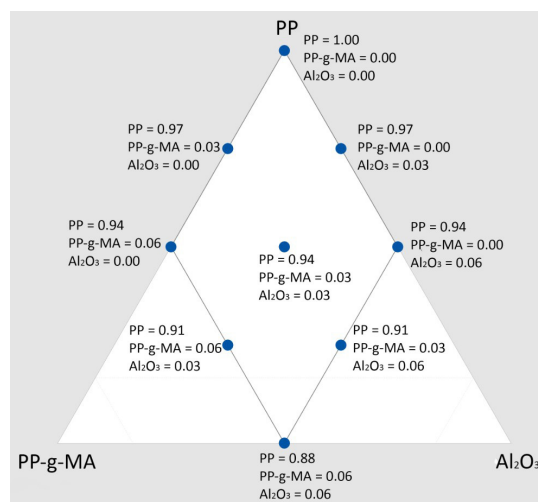
Figure 1. Extreme vertices mixture design region.

Table 1. Composition of PP/PP-g-MA/Al_2O_3 composites.

Sample codes	PP (wt%)	PP-g-MA (wt%)	Al_2O_3 (wt%)
# 1	100	0	0
# 2	88	6	6
# 3	94	0	6
# 4	94	6	0
# 5	97	0	3
# 6	97	3	0
# 7	91	6	3
# 8	91	3	6
# 9	94	3	3

2.2.2. Preparation of PP/PP-g-MA/Al_2O_3 composites

A polypropylene concentrate filled with 8 wt% alumina was prepared in an AX Plástico model 30:32 single-screw extruder with a diameter of 30 mm and a length (L) / diameter (D) ratio = 32. An antioxidant (1% w/w) and a lubricating agent (0.5% w/w) were incorporated into the masterbatch. The temperature profile adopted from the extruder feed to the die was 180/200/200/200/200 °C. The extruder speed

was 35 rpm. The material shaped in the extruder was placed in an oven at 60 °C for 24 hours and subsequently processed and diluted in a Leistritz model ZSE18MAXX-40D co-rotating twin-screw extruder with a rotation speed of 500 rpm, feed rate of 5 kg/h and temperature profile of 200/210/190/190/190/190/200/220/220/230 °C. Dilution was required to reach the proportion of components defined in the experimental mixing design (Table 1).

2.2.3. Preparation of hybrid PP/PP-g-MA/Al₂O₃ /SCF composites

Short carbon fibers (SCF), at concentrations of 10 wt% and 15 wt%, were incorporated into the composite 91/3/6 PP/PP-g-MA/Al$_2$O$_3$ (sample #8), adopted as the matrix of the hybrid composites. The carbon fibers and the matrix were manually mixed and processed in a Leistriz twin-screw extruder, model ZSE18MAXX-40D, with a rotation speed of 500 rpm, a feed rate of 5 kg/h and a temperature profile of 200/210/190/190/190/190/200/220/220/230 °C. After extrusion, the samples were pelletized and placed in an oven at 60 °C for 24 hours. The concentration of Irganox used was 1% of the total mass of each mixture.

2.2.4. Determination of tensile mechanical properties

Tensile properties of all composites were determined using a Shimadzu model AG-X Plus universal testing machine with a 5 kN load cell. The tests were carried out in accordance with ASTM D 638[19], using Type I specimens. A movable crosshead speed of 20 mm/min was used in all determinations. The specimens for the mechanical tests were obtained by injection molding in an Arburg model Allrounder 270 S injection molding machine (IMA/UFRJ). The following injection conditions were used: temperature profile – 160/175/185/195/205 °C; injection pressure – 1200 bar; switching volume – 3 cm³; injection speed - 15 cm³/s; mold temperature – 30 ⁰C; mold cooling time – 30 s; discharge pressure – 600 bar; and discharge time – 2 s. Ten specimens for each sample were used to obtain the mechanical data. The samples' Young's Modulus was determined by the secant method applied at 2% strain. The toughness of the samples was obtained from the area under the stress–strain curves using the following equation[20]:

$$Toughness = \frac{U}{w.t.GL} \qquad (1)$$

Where U is the integrated stress–strain curve area, automatically calculated by the Shimadzu Software, and w, t and GL are the width, thickness and the effective gauge length of the test specimen, respectively.

The Sigma-Plot (version 14) software was used for the statistical analysis of the results. The Shapiro-Wilk test for normality, one-way analysis of variance (ANOVA) and Tukey test were used to determine significant differences between pairs of means of each two samples of data obtained. In cases where data normality was not observed, the Kruskal-Wallis test, one-way analysis of variance and Dunn's nonparametric test were adopted for multiple comparisons of the medians of the data obtained.

2.2.5. Morphological analyses

Scanning electron microscopy (SEM) and transmission electron microscopy (TEM) were used to characterize the materials.

2.2.5.1. SEM analyses

A Hitachi model TM 3000 benchtop scanning electron microscope (SEM), with acceleration voltage of 15 kV was used to evaluate the morphology of the materials. Samples obtained from tensile test specimens were cryogenically fractured in liquid nitrogen and coated with silver in a Bal-Tec SCD 005 Sample Sputter Coater (MCTI/CETEM). Micrographs of the PP/Al$_2$O$_3$ composites were obtained at 500x magnification. Micrographs of PP/carbon fiber composites and hybrid composites were obtained at 200 and 250x magnifications. Different magnifications were used for analysis of composites filled with alumina and carbon fiber due to the difference between the particle sizes of the fillers. The dispersion of alumina in the polymeric matrix was evaluated by energy dispersive spectroscopy (EDS) using an Xflash Min SVE device coupled to the SEM.

2.2.5.2. TEM analyses

An FEI model Tecnai G2 Spirit Twin transmission electron microscope (TEM), (Dimat/Inmetro) with acceleration voltage of 120 KV was used to evaluate the dispersion state of nano α-Al$_2$O$_3$ particles in the 91/3/6 PP/PP-g-MA/Al$_2$O$_3$ composites adopted as a matrix for developing hybrid PP/PP-g-MA/Al$_2$O$_3$/SCF composites. It was necessary to make cuts using a Leica EM UC6 ultramicrotome. Initially, the samples were coated one-by-one with epoxy resin using a silicone mold. The cuts were performed at room temperature, with a diamond knife at an angle of 45° and speed of 1 mm/s, with approximate thickness of 50 nm. The cuts obtained were mounted on 150 mesh copper grids and analyzed by TEM.

3. Results and Discussion

3.1. Tensile mechanical properties of PP and PP/PP-g-MA/Al₂O₃ composites

The tensile mechanical properties of PP and PP/PP-g-MA/Al$_2$O$_3$ composites (Young's modulus, tensile strength and toughness) were determined and evaluated through the response surface methodology. Figures 2 and 3 show Young's modulus and the response surface plot of the tensile elastic modulus of the PP and PP/PP-g-MA/Al$_2$O$_3$ composites.
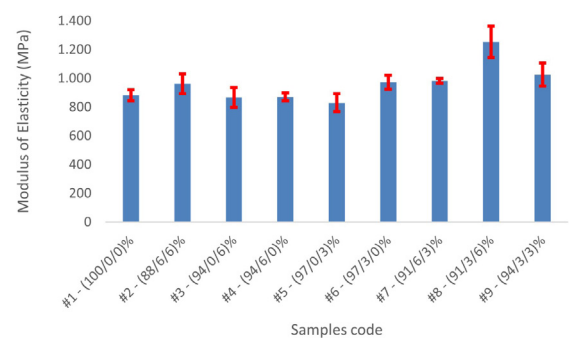
Figure 2. Young's modulus of PP and PP/PP-g-MA/Al$_2$O$_3$ composites.
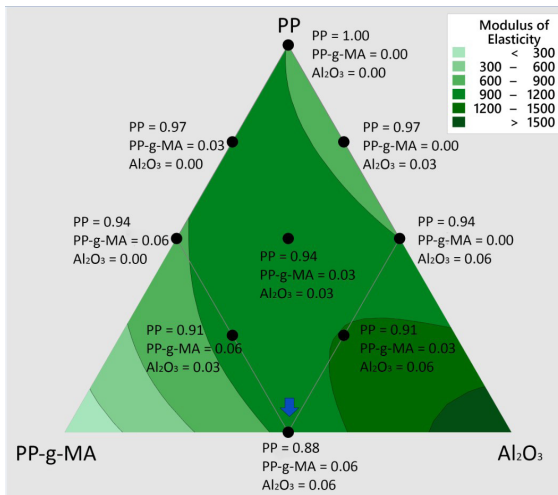
Figure 3. Response surface plot of Young's modulus of PP and PP/PP-g-MA/Al$_2$O$_3$ composites (Minitab - component proportion option).

Alumina is a rigid mineral filler, so it restricts the mobility of polymeric chains. Therefore, an increase in the tensile modulus of the polymer is an expected effect of incorporating this filler in the polypropylene matrix. One-way analysis of variance and the Tukey post-hoc test were used to evaluate the results obtained. Statistical analysis of the data and Figure 2 show there was no significant variation between the PP tensile modulus value and the modulus values of sample #3 (94/0/6 PP/PP-g-MA/Al$_2$O$_3$) and sample #5 (97/0/3 PP/PP-g-MA/Al$_2$O$_3$).

This result was an indication that the filler particles agglomerated, reducing their surface contact area with the matrix.

The poor properties of the PP/nano α-Al$_2$O$_3$ composites can be explained by the agglomeration of alumina nanoparticles in the matrix, acting as failure initiation sites and facilitating the propagation of cracks, as well as the incompatibility of the interface between the non-polar surfaces of polypropylene and the polar alumina[18]. The strategy used to overcome these limitations involves the inclusion of coupling agents, such as silanes and titanium oxide. There are some studies describing their effects on the obtained properties, whereby the better interaction of the filler with the polymer promotes its dispersion in the matrix[21,22].

Arao et al.[3] incorporated PP-g-MA in the polypropylene matrix trying to obtain better interaction between the carbon fibers and polymer. The hybrid composites PP/Al$_2$O$_3$/SCF were prepared in two steps. The first step involved the preparation of PP/PP-g-MA/nano α-Al$_2$O$_3$ nanocomposites to be reinforced in the next step with carbon fibers. The mechanical behavior of polypropylene was improved. In the present work, we prepared PP/PP-g-MA/nano α-Al$_2$O$_3$ composites and determined their tensile properties.

The data obtained showed (Figure 2) that sample #8 (91/3/6 PP/PP-g-MA/Al$_2$O$_3$) had the highest Young's modulus value, 42% higher than that presented by the PP matrix, and 45% higher than the average value of sample #3 (94/0/6 PP/PP-g-MA/Al$_2$O$_3$). The combined action of alumina and compatibilizer promoted an increase in the

stiffness of the polypropylene. The comparison between the average Young's modulus values of sample #5 (97/0/3 PP/PP-g-MA/Al$_2$O$_3$) and sample #9 (94/3/3 PP/PP-g-MA/Al$_2$O$_3$) showed this same effect. Similar results were found by other researchers[21,23-29]. The reason lies in the interaction between the anhydride group of PP-g-MA and the hydroxyl groups of the silica surface[11,12]. The tensile elastic modulus of composites filled with particulate fillers is a function of the contact surface area between the polymer and the particles. Therefore, the results obtained indicated that PP-g-MA promoted the dispersion of alumina particles by increasing this area. However, the comparison between the modulus value of sample #8 (91/3/6 PP/PP-g-MA/Al$_2$O$_3$) and that of sample #2 (88/6/6 PP/PP-g-MA/Al$_2$O$_3$) showed that the lowest concentration used of the compatibilizer (3 wt%) led to obtaining high modulus values. On the other hand, there was no statistically significant difference between the tensile modulus of sample #9 (94/3/3 PP/PP-g-MA/Al$_2$O$_3$) and that of sample #7 (91/6/3 PP/PP-g-MA/Al$_2$O$_3$), which were processed using the same level of alumina and different contents of PP-g-MA. This result may be an indication that the two samples had a similar state of dispersion.

There is some evidence that α-Al$_2$O$_3$ nanoparticles act as polypropylene nucleating agents, favoring the heterogeneous crystallization of this polymer and inducing the formation of small β crystals[18]. Mirjalili et al.[18] showed that nanoparticles promoted the reduction of the spherulite size in relation to that of the polypropylene. However, the crystallinity degree of PP did not change with the development of the nanocomposites.

The surface plot of the elastic modulus (Figure 3) derived from the statistical planning showed the effect of the variation in the composition of the mixture on the mechanical properties of the composites by allowing visual analysis of the results. The surface plot showed that the incorporation of very high levels of Al$_2$O$_3$ or high levels of alumina combined with low contents of PP-g-MA led to high Young's modulus values.

Strong chemical bonding between the nanoparticles and polymeric matrix is mandatory to produce nanocomposites with enhanced mechanical performance. Good dispersion of the fillers, high coverage of the nanoparticles by the matrix (good wetting behavior) and the content of nanofillers incorporated in the polymer are other key factors determining the resulting properties of these materials.

Figures 4 and 5 show the tensile strength results and the plot of the tensile strength response surface of the PP and PP/PP-g-MA/Al$_2$O$_3$ composites. Application of the Shapiro-Wilk normality test to the tensile strength data of PP and PP composites failed ($p < 0.05$). Then the Kruskal-Wallis test, one-way ANOVA and Dunn's post-hoc test were used to evaluate these results.

The data analysis showed that the incorporation of alumina to the 94/0/6 PP/PP-g-MA/Al$_2$O$_3$ composites (sample #3) and to the 97/0/3 PP/PP-g-MA/Al$_2$O$_3$ (sample #5) composites did not promote an increase in the tensile strength of the polymer. The tensile strength of polymeric composites reinforced with particulate fillers is a function of the surface contact area and the degree of adhesion between the filler and matrix[21,30]. Similar results were observed in other studies[21,26,29,31]. The various authors attributed the reduction observed in the

tensile strength of polypropylene with the incorporation of alumina to the low interfacial adhesion, which favors the detachment of the alumina particles from the matrix.
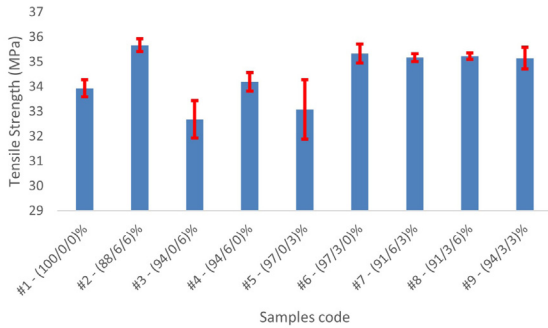
Figure 4. Tensile strength of PP and PP/PP-g-MA/Al_2O_3 composites.
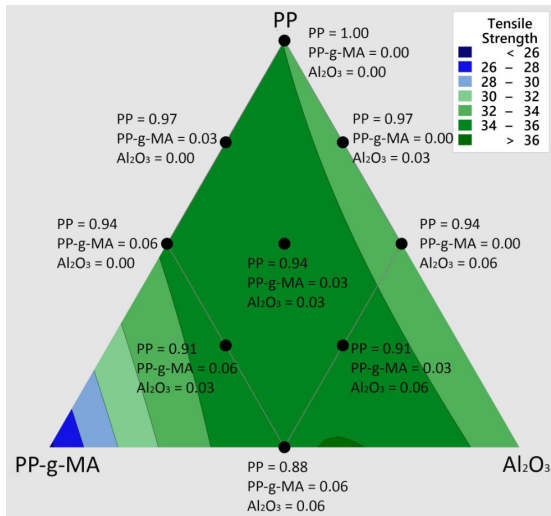
Figure 5. Response surface plot of the tensile strength (Minitab - component proportion option).

Although Al_2O_3, in the concentration range used in this study, did not lead to higher tensile strength values, the joint incorporation of Al_2O_3 and PP-g-MA tended to increase the tensile strength of PP. This increase, however, was only statistically significant when 6 wt% alumina and 6 wt% compatibilizer (sample #2) were added to the polypropylene. PP-g-MA acts as a compatibilizing agent for PP/Al_2O_3 composites, improving the interfacial adhesion between the filler and matrix[32], and according to the modulus of elasticity data obtained, it also promoted the dispersion of the Al_2O_3 particles.

Some studies have reported the use of coupling agents, such as silanes, titanates and anionic dispersants, to improve the interaction between polypropylene and alumina nanoparticles[18,21,22,29]. This increases the tensile strength of the obtained nanocomposites[18,21,29].

Figure 5 shows that the points chosen for the design of mixtures are located within the region with the highest tensile

strength values. The data show that sample #2 (88/6/6 PP/PP-g-MA/Al_2O_3) had the highest average value of tensile strength. However, the median value of tensile strength of sample #2 and those of 94/6/0 PP/PP-g-MA/Al_2O_3 (sample #4), 97/3/0 PP/PP-g-MA/Al_2O_3 (sample #6), 91/6/3 PP/PP-g-MA/Al_2O_3 (sample #7), (91/3/6 PP/PP-g-MA/Al_2O_3) (sample #8) and (94/3/3 PP/PP-g-MA/Al_2O_3) (sample #9) composites were not significantly different. A larger set of data must be obtained and analyzed to achieve greater data accuracy.

Figure 4 also indicates that the incorporation of PP-g-MA to PP tended to promote an increase in the tensile strength of polypropylene. This result can be explained by assuming that PP-g-MA exerts a nucleating effect on the PP matrix, promoting an increase in crystallinity and an improvement in the mechanical properties of the polymer[33].

In general, the elongation at break decreased with increasing stiffness of the materials, due to the lower deformability of the rigid interface between fillers and the polymeric matrix. This effect can cause a reduction in the ductility and toughness of nanocomposites[18].

Figures 6 and 7 show the toughness data of the materials under study and the response surface plot of the toughness of PP and PP/PP-g-MA/Al_2O_3 composites. The Kruskal-Wallis test, one-way ANOVA and Dunn's post-hoc test were used to evaluate these results.
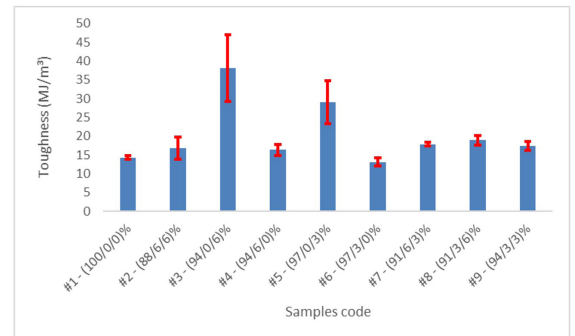
Figure 6. Toughness of PP and PP/PP-g-MA/Al_2O_3 composites.
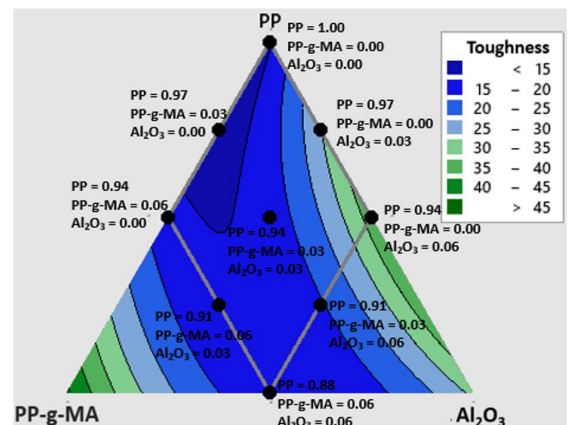
Figure 7. Response surface plot of toughness (Minitab - component proportion option).

Inspection of Figure 6 shows that the toughness values of samples filled with alumina without using the compatibilizer, sample #3 (94/0/6 PP/PP-g-MA/Al$_2$O$_3$) and sample #5 (97/0/3 PP/PP-g-MA/Al$_2$O$_3$), respectively presented relatively high standard deviations. As previously mentioned, PP-g-MA is essential to promote the dispersion of alumina in the PP matrix, leading to obtaining homogeneous samples. Statistical analysis of the data showed that these two samples had toughness values significantly higher than that presented by PP and there was no significant difference between the median values of these two samples.

Pedrazolli et al.[24], in a study of the properties of boehmite alumina nanoparticle/PP composites, verified that the elongation at break increased, reaching a maximum with filler content of 2.5 wt%. This result was explained by the failure mode effect, in which particles debond first, followed by coalescence of voids associated with matrix fibrillation.

A possible explanation for the results obtained in the present work involves this failure mode, in which due to the low concentrations of alumina used, the voids caused during the detachment process of the filler from the matrix became further from each other. The presence of voids alters the state of stress within the material in close proximity to the particles, relieving the stress and reducing the tendency for crack propagation. Thus, a mechanism involving the formation of shear bands would occur, causing the material to absorb a greater amount of energy. In any case, this effect would decrease with increasing alumina content, since the average interparticle distance would decrease with increasing alumina content[20]. The high standard deviations associated with toughness determination make data interpretation difficult.

An improvement in PP toughness was not obtained by the combined action of PP-g-MA and Al$_2$O$_3$. The stiffer interface between polymer and filler was responsible for this result.

Figure 7 shows that the points chosen for the design of mixtures are located outside the region of higher toughness values, indicating that the incorporation of high levels of Al$_2$O$_3$ leads to obtaining PP/Al$_2$O$_3$ composites with toughness values higher than those of the PP matrix and composite sample #5 (97/0/3 PP/PP-g-AM/Al$_2$O$_3$). This result is in line with the data presented in Figure 6.

3.2. Morphological analysis of PP/PP-g-MA/ Al$_2$O$_3$ composites

SEM/energy dispersive spectroscopy (EDS) micrographs of the composites were used to evaluate the dispersion and distribution of Al$_2$O$_3$ in the PP/PP-g-MA/Al$_2$O$_3$ composites.

Sample #8 had the highest Young's modulus value and sample #2 had the highest tensile strength value.

Figure 8 shows the SEM/EDS micrographs of composite samples #3 (94/0/6 PP/PP-g-MA/Al$_2$O$_3$) and #8 (91/3/6 PP/PP-g-MA/Al$_2$O$_3$), and Figure 9 shows the micrographs of
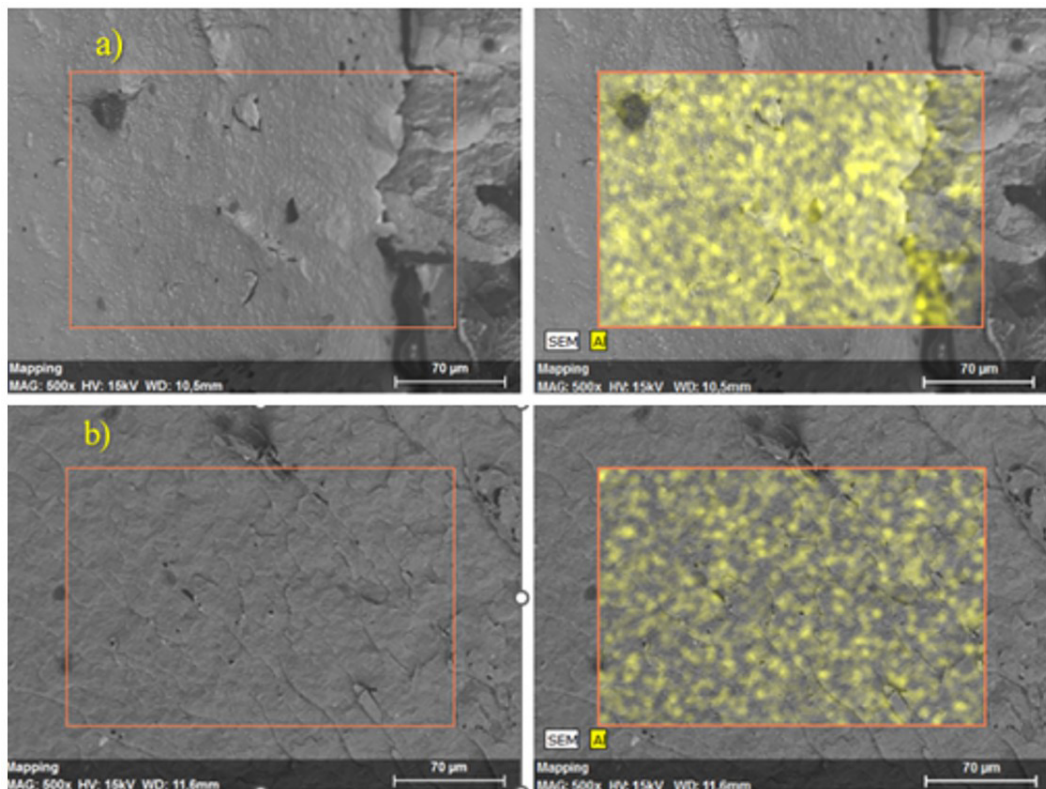
Figure 8. SEM/EDS micrographs of PP/Al$_2$O$_3$ composite samples #3 and #8.

SEM micrographs: (a) 94/0/6 PP /PP-g-MA/Al$_2$O$_3$ composites at 500x magnification; (b) 91/3/6 PP /PP-g-MA /Al$_2$O$_3$ composites at 500x magnification.
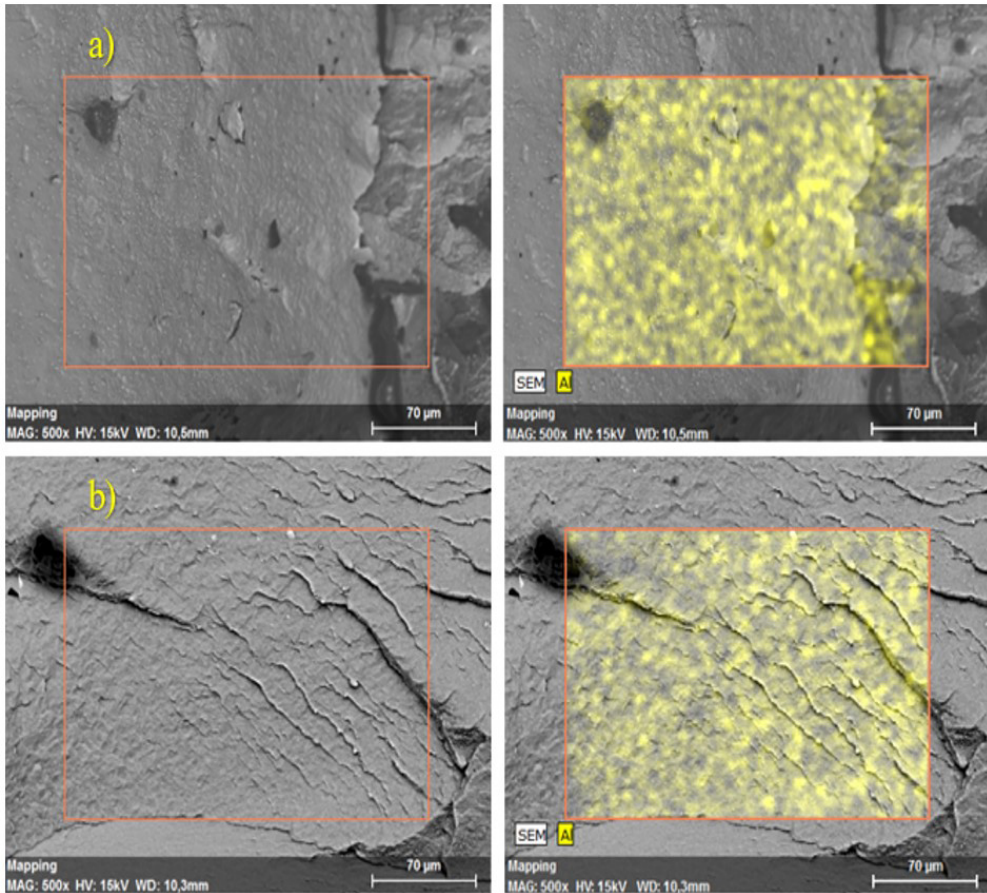
Figure 9. SEM/EDS micrographs of PP/Al$_2$O$_3$ composite samples #3 and #2.

SEM micrographs: (a) 94/0/6 /PP-g-MA/Al$_2$O$_3$ composites at 500x magnification; (b) 88/6/6 PP /PP-g-MA /Al$_2$O$_3$ composites at 500x magnification.

94/0/6 PP/PP-g-MA/Al$_2$O$_3$ (sample #3) and 88/6/6 PP/PP-g-MA/Al$_2$O$_3$ (sample #2).

The micrographs show there was good dispersion and distribution of the alumina in the polypropylene matrix, although there are some regions where larger grains of alumina are evident (points with a more intense yellow). This result indicates there was some agglomeration of the alumina due to the existing Van der Waals force of attraction between the alumina particles[34]

Pérez et al.[32], evaluating the effect of rigid fillers on fracture and failure of PP-based composites, found that the agglomerates present in composites processed with PP-g-MA were significantly smaller than those in composites processed without the coupling agent.

The micrographs (Figures 8 and 9) obtained in the present work also show that, with the incorporation of PP-g-MA, the composites obtained had a finer morphology. The presence of agglomerates is still evident, but their sizes are smaller, and the nanoparticles are no longer so distinguishable from the matrix. In Figure 9, this effect is more evident.

The compatibilizer promoted a reduction of voids caused by the removal of Al$_2$O$_3$ nanoparticles, indicating that the interfacial adhesion between the polymer and the filler was improved.

These results corroborate those obtained in the tensile tests of these samples, where higher average Young's modulus and tensile strength values were obtained with the incorporation of PP-g-MA in the PP/Al$_2$O$_3$ mixtures.

The dispersion of nanofillers in the polymer matrix is one of the most important factors to obtain composites with high mechanical performance[18]. Mirjalili et al.[18] attributed the decrease in tensile strength of PP/nano α-Al$_2$O$_3$ particle composites to the presence of large agglomerates. The authors found that the use of an anionic dispersant exerted a significant effect on the size of the nanoparticle agglomerates.

Figure 10 shows the TEM micrographs of the 91/3/6 PP/PP-g-MA/Al$_2$O$_3$ nanocomposite (sample #8). The images show very good dispersion of the nanoparticles, although the presence of some nanosized clusters is evident. This result is in agreement with the high Young's modulus of this sample. The dispersion of nanoparticles is also a requirement to obtain high tensile strength values. However, the tensile strength is also a function of a strong interface between filler and matrix[30]. Figure 8 shows that the interfacial strength between the nanoparticles and PP was not strong enough to promote a significant increase in this property.

The evaluation of the TEM images of the other nanocomposites obtained is in progress.
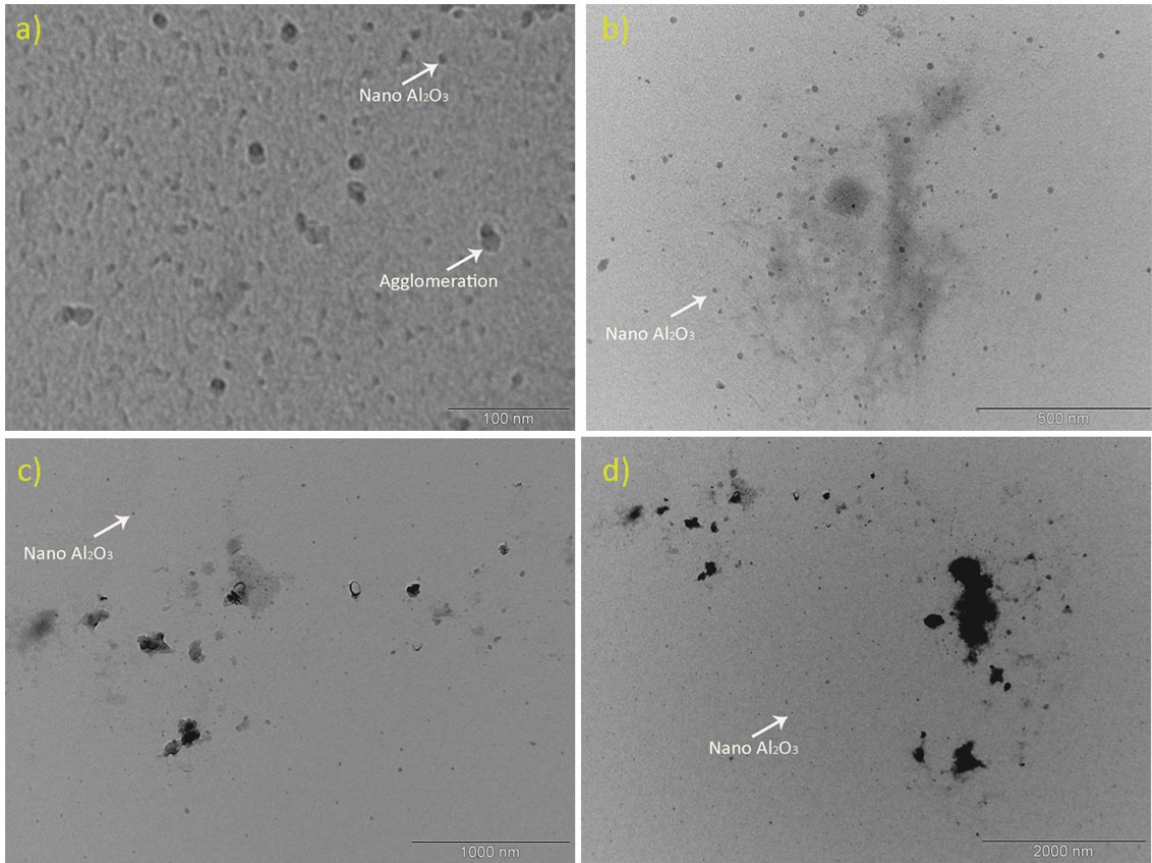
Figure 10. TEM micrographs of 91/3/6 PP/PP-g-MA/Al$_2$O$_3$ nanocomposite at different magnifications. TEM observations: (a) 100 nm; (b) 500 nm; (c) 1000 nm; (d) 2000 nm.

3.3. Mechanical properties of PP/PP-g-MA/ Al$_2$O$_3$/SCF hybrid composites

The choice of nanocomposites as matrices for thermoplastic composites reinforced with carbon fibers does not only rest on the best properties of the matrix. Small nanoparticles fit well between the fibers and improve the interfacial adhesion between the fibers and matrix, leading to higher interfacial shear strength (IFSS) values[3].

The IFSS between a carbon fiber and PP is very small, preventing the attainment of high strength. Some studies[3,10-12] have reported the incorporation of nanoparticles and low levels of compatibilizers such as PP-g-MA in PP, in order to obtain hybrid PP composites with high strength. The incorporation of PP-g-MA in the matrix has positive effects on the covering ratio of the fibers and also on the reduction of fiber length during processing.

Arao et al.[3] reported that the incorporation of nanoparticles of alumina, silica and carbon nanotubes (CNT) in polypropylene improved the IFSS and led to superior mechanical properties.

The nanocomposite sample #8 (91/3/6 PP/PP-g-MA/Al$_2$O$_3$), due to its good mechanical and morphological properties, was initially chosen as a matrix for the development of hybrid composites.

Short carbon fibers at the levels of 10 and 15 wt% were incorporated in the matrix.

Figures 11, 12 and 13 present the results obtained for modulus of elasticity, tensile strength and toughness of hybrid composites. One-way analysis of variance and the Tukey post-hoc test were used to evaluate the results.
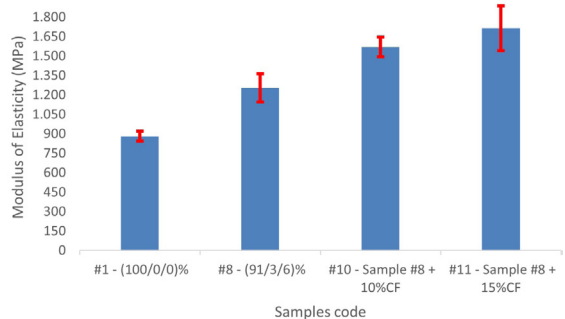
Figure 11. Young's modulus of PP, sample #8 (91/3/6 PP/Al$_2$O$_3$) and PP/PP-g-MA/Al$_2$O$_3$/SCF hybrid composites.

Figure 11 shows that the incorporation of carbon fibers in the matrix produced higher tensile modulus. The incorporation of higher level of fibers tended to promote an increase in the modulus, since on a statistical basis, sample #10 and sample #11 were equivalent.

The hybrid composites obtained showed increases in the tensile modulus of about 25% and 37% in relation to sample

#8. In relation to polypropylene, these increases were 78% and 95%, respectively, resulting from the greater stiffness of the carbon fiber.
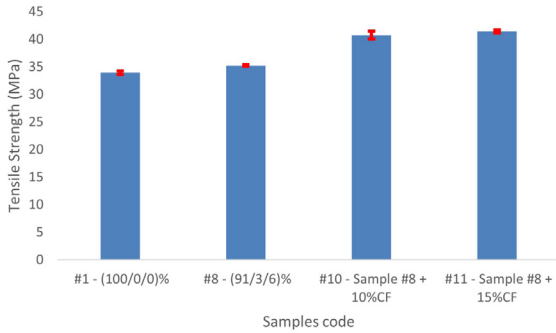
Figure 12. Tensile strength of PP, sample #8 (91/3/6 PP/PP-g-Al$_2$O$_3$) and PP/PP-g-MA/Al$_2$O$_3$/SCF hybrid composites.

Figure 12 shows that the incorporation of 10 wt% of carbon fiber in the matrix was sufficient to cause an increase of around 16% in tensile strength. In relation to PP, the increase in tensile strength was around 20%. This increase in tensile strength occurred due to the more efficient transfer of tensile stress between the reinforcement and the polymeric matrix, caused by the addition of carbon fibers[35].

Short carbon fibers do no contribute to increase the tensile strength of polymers. The high shear that occurs in the processing of composites in a twin-screw extruder causes fiber breakage. Thus, the ends of the fibers, due to their shorter length, act more effectively as stress concentrators. The incorporation of PP-g-MA contributes to better mechanical performance of the composites. PP-g-MA improves final fiber length, fiber covering properties and increases the interfacial shear stress (IFFS). In addition, nanoparticles also helped enhance the adhesion between polymer and fibers[3].

The reduction in toughness of the hybrid composites (Figure 13) was around 82%, in relation to the value of the matrix. In relation to polypropylene, this reduction was around 75%.

This drastic reduction of toughness was not expected, since in another study the incorporation of nanofillers in polymeric matrices increased the crack resistance of the materials. Nanofillers in general act as nucleating agents for polypropylene, reducing the size of spherulites[3]. The increase in the stiffness may explain our results. The incorporation of a lower carbon fiber content in the matrix should be evaluated to avoid such a significant decrease in toughness, without compromising the high values of modulus of elasticity and tensile strength obtained.
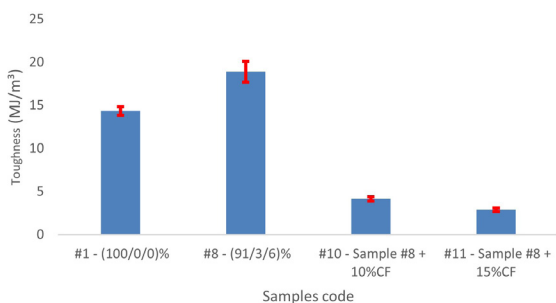
Figure 13. Toughness of PP, sample #8 (91/3/6 PP/PP-g-MA/Al$_2$O$_3$) and PP/PP-g-MA/Al$_2$O$_3$/SCF hybrid composites.

Junaedi et al.[36] reported that the toughness of polypropylene decreases with the incorporation of short carbon fibers in the polymer. The authors concluded that a decrease in strain at break (ductility) is one of the major drawbacks in SCF-reinforced thermoplastic composites. In another work[37] on polypropylene composites reinforced with fibers, the authors showed that the incorporation of any content of fiber in polypropylene resulted in a decrease in fracture resistance, causing early failure of the composite.

3.4. Morphological analysis of PP/PP-g-MA/ Al$_2$O$_3$/SCF hybrid composites

Figures 14 and 15 show the micrographs of the PP/PP-g-MA/Al$_2$O$_3$/SCF hybrid composites.
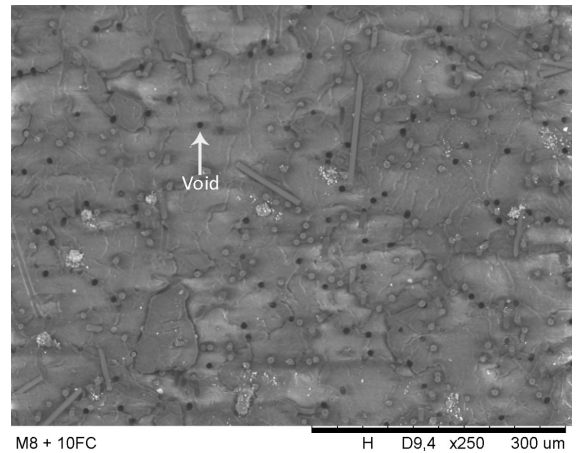
Figure 14. SEM micrograph of the hybrid composite reinforced with 10 wt% CF.
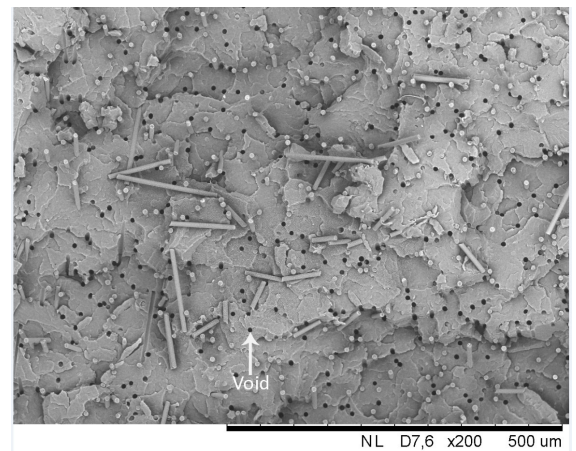
Figure 15. SEM micrograph of the hybrid composite reinforced with 15 wt% CF.

The micrographs reveal several voids (holes) caused by the removal of carbon fibers during the fracture, and the incorporation of a higher level of fiber (15 wt%) accentuated this effect. The carbon fibers have a smooth and clean appearance and are overturned in the images, which shows the weak interfacial adhesion between the carbon fibers

and the polypropylene matrix[38-40]. The incorporation of carbon fibers in sample #8 (91/3/6 PP-g-MA/Al_2O_3) caused a significant reduction in toughness. The weak adhesion between PP and SCF, as well as the reduction of the fibers' length during processing, can explain the low toughness values of the hybrid composites.

The poor interfacial adhesion, however, did not prevent an increase in tensile strength from approximately 35 MPa to 41 MPa when carbon fiber was added at both 10 and 15 wt% levels in the matrix. Surface treatment of the alumina by using other coupling agents can be performed to promote better interaction of the matrix with the carbon fiber, in addition to minimizing the formation of agglomerates, since larger particles usually cause a reduction in toughness[41]. The use of matrices with a higher maleic anhydride content, such as sample #2 (88/6/6 PP/PP-g-MA/Al_2O_3), led to better results. Perhaps the maleic anhydride groups were consumed in the reaction between PP-g-MA and nanoparticles.

Another hypotheses to solve this problem involves the incorporation of a lower carbon fiber content in the matrix, and the use of matrices with higher toughness, such as sample #3 (94/0/6 PP/PP-g-MA/Al_2O_3) and sample #5 (97/0/3 PP/PP-g-MA/Al_2O_3), which had the highest toughness values, 38.12 MJ/m^3 and 29 MJ/m^3, respectively.

4. Conclusions

Nanocomposite sample #8 (91/3/6 PP/PP-g-MA/Al_2O_3) was chosen as matrix for the development of hybrid composites due to its good mechanical and morphological properties.

The incorporation of 10 and 15 wt% short carbon fibers in this matrix gave rise to composites, with modulus of elasticity and tensile strength significantly higher than those presented by the matrix. These good mechanical properties, however, were obtained at the expense of greatly reduced toughness. Therefore, the materials obtained can be used in applications that require lightness, high productivity, stiffness and strength, and in which toughness under application of a static load is not required. The micrographs of the PP/Al_2O_3 composites showed there was good dispersion and distribution of alumina in the polypropylene matrix. However, larger alumina grains were detected, indicating there was alumina agglomeration in some regions. The micrographs also showed that the use of PP-g-MA as a compatibilizer in PP/Al_2O_3 composites promoted better alumina dispersion and better interfacial adhesion between alumina and polypropylene, resulting in tensile properties superior to those of polypropylene. The TEM images showed that the dispersion of the alumina particles occurred on nanometric size scale. The PP-g-MA and the nanoparticles must have promoted better interfacial adhesion between the carbon fibers and the polypropylene and greater coverage of the fibers by the matrix, as demonstrated by the increase in the modulus and tensile strength of the hybrid composites in relation to the matrix.

5. Acknowledgments

6. References

1. Khanam PN, AlMaadeed MA. Processing and characterization of polyethylene-based composites. Adv Manuf: Polym Compos Sci. 2015;1(2):63-79. http://dx.doi.org/10.1179/2055035915Y.0000000002.

2. Culbert S, Luo C, Park A, Spitzer B, Lynch J, Chang E. Development and characterization of plastic composites. 2018 IEEE MIT Undergraduate Research Technology Conference (URTC); 2018; Cambridge. Proceedings. USA: IEEE; 2018. p. 1-4.

3. Arao Y, Yumitori S, Suzuki H, Tanaka T, Tanaka K, Katayama T. Mechanical properties of injection-molded carbon fiber/polypropylene composites hybridized with nanofillers. Compos, Part A Appl Sci Manuf. 2013;55:19-26. http://dx.doi.org/10.1016/j.compositesa.2013.08.002.

4. Arao Y, Yumitori S, Suzuki H, Tanaka T, Tanaka K, Katayama T. Hybrid effects on mechanical properties of injection molded nano-hybrid composites. In: ECCM 2012 - Composites at Venice, Proceedings of the 15th European Conference on Composite Materials; 2012; Italy. Proceedings. Venice: JEC; 2012. p. 24-8.

5. Hassanzadeh-Aghdam MK, Mahmoodi MJ, Jamali J, Ansari R. A new micromechanical method for the analysis of thermal conductivities of unidirectional fiber/CNT-reinforced polymer hybrid nanocomposites. Compos, Part B Eng. 2019;175:107137. http://dx.doi.org/10.1016/j.compositesb.2019.107137.

6. Junaedi H, Baig M, Dawood A, Albahkali E, Almajid A. Mechanical and physical properties of short carbon fiber and nanofiller-reinforced polypropylene hybrid nanocomposites. Polymers (Basel). 2020;12(12):2851. http://dx.doi.org/10.3390/polym12122851.

7. Paszkiewicz S, Pypeć K, Irska I, Piesowicz E. Functional polymer hybrid nanocomposites based on polyolefins: a Review. Processes (Basel). 2020;8(11):1475. http://dx.doi.org/10.3390/pr8111475.

8. Kaybal HB, Ulus H, Demir O, Şahin ÖS, Avci A. Effects of alumina nanoparticles on dynamic impact responses of carbon fiber reinforced epoxy matrix nanocomposites. Eng Sci Technol an Int J. 2018;21(3):399-407. http://dx.doi.org/10.1016/j.jestch.2018.03.011.

9. Chang HW, Smith RP, Li SK, Neumann AW. Wettability of reinforcing fibers. In: Ishida H, Kumar G, editors. Molecular characterization of composite interfaces. Berlin: Springer; 1985. p. 413-21.

10. Pérez-Rocha D, Morales-Cepeda AB, Navarro-Pardo F, Lozano-Ramírez T, LaFleur PG. Carbon fiber composites of pure polypropylene and maleated polypropylene blends obtained from injection and compression moulding. Int J Polym Sci. 2015;2015:1-8. http://dx.doi.org/10.1155/2015/493206.

11. Kim JS, Kim DH. Compatibilizing effects of maleic anhydride-grafted-polypropylene (pp) on long carbon fiber-reinforced PP composites. J Thermoplast Compos Mater. 2014;28(11):1599-611. http://dx.doi.org/10.1177/0892705714563562.

12. Randall JD, Stojcevski F, Djordjevic N, Hendlmeier A, Dharmasiri B, Stanfield MK, et al. Carbon fiber polypropylene interphase modification as a route to improved toughness. Compos, Part A Appl Sci Manuf. 2022;159:107001. http://dx.doi.org/10.1016/j.compositesa.2022.107001.

13. Boublia A, Lebouachera SE, Haddaoui N, Guezzout Z, Ghriga MA, Hasanzadeh M, et al. State-of-the-art review on recent advances in polymer engineering: modeling and optimization through response surface methodology approach. Polym Bull. 202;80:5999-6031. http://dx.doi.org/10.1007/s00289-022-04398-6.

14. Sun L, Wan S, Yu Z, Wang L. Optimization and modeling of preparation conditions of tio2 nanoparticles coated on hollow glass microspheres using response surface methodology. Separ Purif Tech. 2014;125:156-62. http://dx.doi.org/10.1016/j.seppur.2014.01.042.

15. Ghelich R, Jahannama MR, Abdizadeh H, Torknik FS, Vaezi MR. Central Composite Design (CCD)-response surface methodology (RSM) of effective electrospinning parameters on PVP-B-HF hybrid nanofibrous composites for synthesis of HFB2-based composite nanofibers. Compos, Part B Eng. 2019;166:527-41. http://dx.doi.org/10.1016/j.compositesb.2019.01.094.

16. Chelladurai SJ, K M, Ray AP, Upadhyaya M, Narasimharaj V. Optimization of process parameters using response surface methodology: a review. Mater Today Proc. 2021;37:1301-4. http://dx.doi.org/10.1016/j.matpr.2020.06.466.

17. ASTM: American Society for Testing and Materials. ASTM D1238: Standard test method for melt flow rates of the thermoplastic by extrusion plastometer. Philadelphia: ASTM; 2010.

18. Mirjalili F, Chuah L, Salahi E. Mechanical and morphological properties of polypropylene/nano α-AL2O$_3$ composites. ScientificWorldJournal. 2014;2014:718765. http://dx.doi.org/10.1155/2014/718765.

19. ASTM: American Society for Testing and Materials. ASTM D638: Standard test method for tensile properties of plastics. Philadelphia: ASTM; 2003.

20. Lins SA, Rocha MC, d'Almeida JR. Mechanical and thermal properties of high-density polyethylene/alumina/glass fiber hybrid composites. J Thermoplast Compos Mater. 2018;32(11):1566-81. http://dx.doi.org/10.1177/0892705718797391.

21. Akil HM, Lily N, Razak JA, Ong H, Ahmad ZA. Effect of various coupling agents on properties of alumina-filled PP composites. J Reinf Plast Compos. 2006;25(7):745-59. http://dx.doi.org/10.1177/0731684406062068.

22. Truong LT, Larsen Å, Holme B, Diplas S, Hansen FK, Roots J, et al. Dispersibility of silane-functionalized alumina nanoparticles in syndiotactic polypropylene. Surf Interface Anal. 2010;42(6-7):1046-9. http://dx.doi.org/10.1002/sia.3166.

23. Li B, Li R, Xie Y. Properties and effect of preparation method of thermally conductive polypropylene/aluminum oxide composite. J Mater Sci. 2016;52(5):2524-33. http://dx.doi.org/10.1007/s10853-016-0546-8.

24. Pedrazzoli D, Khumalo VM, Karger-Kocsis J, Pegoretti A. Thermal, viscoelastic and mechanical behavior of polypropylene with synthetic boehmite alumina nanoparticles. Polym Test. 2014;35:92-100. http://dx.doi.org/10.1016/j.polymertesting.2014.03.003.

25. Pedrazzoli D, Tuba F, Khumalo VM, Pegoretti A, Karger-Kocsis J. Mechanical and rheological response of polypropylene/boehmite nanocomposites. J Reinf Plast Compos. 2013;33(3):252-65. http://dx.doi.org/10.1177/0731684413505787.

26. Mai K, Li Z, Qiu Y, Zeng H. Mechanical properties and fracture morphology of Al(OH)3/polypropylene composites modified by PP grafting with acrylic acid. J Appl Polym Sci. 2001;80(13):2617-23. http://dx.doi.org/10.1002/app.1373.

27. Silva GDA, Alves KGB, Almeida YB, Sanguinetti RA, Yadava YP. Effect of alumina ceramic powder dispersion on mechanical properties of polypropylene polymers. Mater Sci Forum. 2012;727-728:1729-33. http://dx.doi.org/10.4028/www.scientific.net/MSF.727-728.1729.

28. Streller RC, Thomann R, Torno O, Mülhaupt R. Isotactic poly(propylene) nanocomposites based upon Boehmite

29. Zhao H, Li RK. Crystallization, mechanical, and fracture behaviors of spherical alumina-filled polypropylene nanocomposites. J Polym Sci, B, Polym Phys. 2005;43(24):3652-64. http://dx.doi.org/10.1002/polb.20654.

30. Eiras D, Pessan LA. Mechanical properties of polypropylene/calcium carbonate nanocomposites. Mater Res. 2009;12(4):517-22. http://dx.doi.org/10.1590/S1516-14392009000400023.

31. Plentz RS, Miotto M, Schneider EE, Forte MM, Mauler RS, Nachtigall SM. Effect of a macromolecular coupling agent on the properties of aluminum hydroxide/PP composites. J Appl Polym Sci. 2006;101(3):1799-805. http://dx.doi.org/10.1002/app.23558.

32. Pérez E, Alvarez V, Pérez CJ, Bernal C. A comparative study of the effect of different rigid fillers on the fracture and failure behavior of polypropylene based composites. Compos, Part B Eng. 2013;52:72-83. http://dx.doi.org/10.1016/j.compositesb.2013.03.035.

33. Seo Y, Kim J, Kim KU, Kim YC. Study of the crystallization behaviors of polypropylene and maleic anhydride grafted polypropylene. Polymer (Guildf). 2000;41(7):2639-46. http://dx.doi.org/10.1016/S0032-3861(99)00425-5.

34. Rasana N, Jayanarayanan K. Polypropylene/short glass fiber/nanosilica hybrid composites: evaluation of morphology, mechanical, thermal, and transport properties. Polym Bull. 2017;75(6):2587-605. http://dx.doi.org/10.1007/s00289-017-2173-1.

35. Yamamoto G, Onodera M, Koizumi K, Watanabe J, Okuda H, Tanaka F, et al. Considering the stress concentration of fiber surfaces in the prediction of the tensile strength of unidirectional carbon fiber-reinforced plastic composites. Compos, Part A Appl Sci Manuf. 2019;121:499-509.http://dx.doi.org/10.1016/j.compositesa.2019.04.011.

36. Junaedi H, Albahkali E, Baig M, Dawood A, Almajid A. Ductile to brittle transition of short carbon fiber-reinforced polypropylene composites. Adv Polym Technol. 2020;2020:1-10. http://dx.doi.org/10.1155/2020/6714097.

37. Doddalli Rudrappa S, Yellampalli Srinivasachar V. Significance of the type of reinforcement on the physicomechanical behavior of short glass fiber and short carbon fiber-reinforced polypropylene composites. Eng Reports. 2020;2(2):e12098. http://dx.doi.org/10.1002/eng2.12098.

38. Pedrazzoli D, Pegoretti A. Hybridization of short glass fiber polypropylene composites with nanosilica and graphite nanoplatelets. J Reinf Plast Compos. 2014;33(18):1682-95. http://dx.doi.org/10.1177/0731684414542668.

39. Xie H-Q, Zhang S, Xie D. An efficient way to improve the mechanical properties of polypropylene/short glass fiber composites. J Appl Polym Sci. 2005;96(4):1414-20. http://dx.doi.org/10.1002/app.21575.

40. Zebarjad SM, Bagheri R, Seyed Reihani SM, Forunchi M. Investigation of deformation mechanism in polypropylene/glass fiber composite. J Appl Polym Sci. 2003;87(13):2171-6. http://dx.doi.org/10.1002/app.11609.

41. Sahebian S, Zebarjad SM, Sajjadi SA, Sherafat Z, Lazzeri A. Effect of both uncoated and coated calcium carbonate on fracture toughness of HDPE/Caco3 nanocomposites. J Appl Polym Sci. 2007;104(6):3688-94. http://dx.doi.org/10.1002/app.25644.

nanofillers. Macromol Mater Eng. 2008;293(3):218-27. http://dx.doi.org/10.1002/mame.200700354.